

Implementation of Field Oriented Speed Sensorless Control of Induction Motor Drive

R. Gunabalan¹ and V. Subbiah²

¹School of Electrical and Electronics Engineering, VIT University, Chennai, TamilNadu, INDIA

²Department of Electrical and Electronics Engineering, PSG College of Technology, Coimbatore, TamilNadu, INDIA

Abstract: This paper focuses the hardware realization and implementation of speed-sensorless field oriented control of induction motor drive. For speed sensorless operation, natural observer is applied to estimate the stator currents, rotor fluxes, load torque and rotor speed because of its simple structure and no direct feedback. The configuration of the natural observer is comparable to and as well as its feature is identical to the induction motor. State space model is applied to both the estimator and the induction motor. Load torque adaptation is provided to estimate the load torque and, speed is estimated from the torque, rotor fluxes and stator currents. Direct field oriented sensorless vector control scheme is used and the rotor angle is calculated from the estimated rotor fluxes. Simulations as well as experimental results are presented for various speed and load conditions to demonstrate the performance of natural observer in sensorless vector control applications.

Keywords: Induction motor, DSP processor, observer, sensorless control, simulation

1. Introduction

Induction motors are favoured for very large drives because of the boundaries of commutation and rotor speed in dc drives. The induction motor is in fact 'brushless' and can work with simple controls without a shaft position transducer. Induction motor control can be classified into two types: scalar control and vector control.

In scalar control [1], the magnitude of the control variable is varied and it disregards the coupling effect in the machine. The most popular method is V/f control, which adjusts the constant volt per hertz of the stator voltage to keep the stator flux constant. The dynamic performance of V/f control is unsatisfactory because of temperature and saturation effect. Recent developments in fast switching power semiconductor devices and powerful digital signal processors made advanced control techniques of induction motors.

The vector control is introduced in the beginning of 1970s. The vector control consists of controlling the stator currents represented by a vector. This control is based on transforming a three phase time and frequency dependent system into a two co-ordinate (d and q axes) time invariant system. These projections lead to a structure similar to that of a separately excited dc motor control.

Vector control is also called as Field Oriented Control (FOC). Generally, two types of field oriented control schemes are available. 1. Direct field oriented control 2. Indirect field oriented control. In the direct scheme, the instantaneous position of rotor flux (θ_e) has to be measured using flux sensors. This adds to the cost and complexity of the drive system. In the indirect scheme, a model of induction motor is required to calculate the reference angular slip frequency that has to be added to the measured rotor speed. The sum is integrated to calculate the instantaneous position of the rotor flux. Indirect field orientation is more sensitive to parameters values inaccuracy than direct field orientation. The value of the rotor time constant (L_r/R_r) is used in the slip frequency calculation and is sensitive to temperature and flux level. The need of special position incremental encoder is another disadvantage of the method. To avoid these complications, different algorithms are projected, to estimate both the rotor flux

vector and/or rotor shaft speed. The induction motor drives without mechanical speed sensors have the attractions of low cost, high reliability and reduce the size and the lack of additional wiring for sensors or devices mounted on the shaft. Nowadays, a number of adaptive observer design techniques are available for speed and flux estimation. The standard speed estimators are Luenberger observer [2] – [7], Extended Kalman Filter (EKF) [8] – [13], Model Reference Adaptive System (MRAS) [14] – [18], natural observer [19], load torque observer [20]-[21], sliding mode observer [22] – [23] etc.

The selection of the observer gain constant (K) is difficult in Luenberger observer. The initial selection of noise covariance matrices is not easy in EKF and subsequently the algorithm is complicated. The number of inputs in EKF and Luenberger observer is different to the number of inputs to the induction motor since they utilize output feedback. The above difficulties are overcome by introducing natural observer for estimating the speed and also the load torque.

The paper is organized as follows: Chapter 2 discusses the concepts of natural observer. The simulation results are presented in chapter 3. Hardware circuits and results are presented in chapter 4 and are concluded in chapter 5.

2. Mathematical Model of Natural Observer

The structure and features of the natural observer are identical to the induction motor for the given supply voltage and load torque. The major difference between natural and conventional observer is that there is no external feedback and faster convergence rate. As a result, the speed estimation follows the speed changes simultaneously. Its dynamic behavior is exactly the same as the motor and load torque adaptation is used to estimate the load torque from the active power error. Fourth order induction motor model in stator flux oriented reference frame is used to estimate the speed, where dq -axes stator currents and rotor fluxes are selected as state variables. The induction motor is represented in stationary reference frame by the following state equations:

$$\frac{dx}{dt} = AX + BV_s \tag{1}$$

$$Y = CX \tag{2}$$

where,

$$A = \begin{bmatrix} -\left(R_s + R_r \left(\frac{L_m}{L_r}\right)^2\right) & 0 & \frac{L_m}{\sigma L_s L_r \tau_r} & \frac{\omega_r L_m}{\sigma L_s L_r} \\ 0 & -\left(R_s + R_r \left(\frac{L_m}{L_r}\right)^2\right) & \frac{-\omega_r L_m}{\sigma L_s L_r} & \frac{L_m}{\sigma L_s L_r \tau_r} \\ \frac{L_m}{\tau_r} & 0 & \frac{-1}{\tau_r} & -\omega_r \\ 0 & \frac{L_m}{\tau_r} & \omega_r & \frac{-1}{\tau_r} \end{bmatrix}$$

$$B = \begin{bmatrix} \frac{1}{\sigma L_s} & 0 \\ 0 & \frac{1}{\sigma L_s} \\ 0 & 0 \\ 0 & 0 \end{bmatrix} \quad C = \begin{bmatrix} 1 & 0 & 0 & 0 \\ 0 & 1 & 0 & 0 \end{bmatrix}$$

$\sigma = 1 - \frac{L_m^2}{L_s L_r}$ - leakage coefficient

$$X = [i_{ds}^s \quad i_{qs}^s \quad \varphi_{dr}^s \quad \varphi_{qr}^s]^T$$

$$Y = [i_{ds}^s \quad i_{qs}^s] = i_s$$

$$V_s = [V_{ds}^s \quad V_{qs}^s]^T$$

Implementation of Field Oriented Speed Sensorless

L_s, L_r – stator and rotor self inductance respectively (H)

L_m – mutual inductance (H)

τ_r –rotor time constant = $\frac{L_r}{R_r}$

ω_r –motor angular velocity (rad/s)

The block diagram representation of natural observer is shown in Figure 1 and the observer state equations are as follows:

$$\frac{d\hat{X}}{dt} = \hat{A}\hat{X} + BV_s \quad (3)$$

$$\hat{Y} = C\hat{X} \quad (4)$$

$$\hat{X} = [\hat{i}_{ds}^s \quad \hat{i}_{qs}^s \quad \hat{\phi}_{dr}^s \quad \hat{\phi}_{qr}^s]^T$$

$$\hat{Y} = [\hat{i}_{ds}^s \quad \hat{i}_{qs}^s]^T = \hat{i}_s$$

where, “^” represents the estimated quantities.

The load torque is estimated from the active power error by the following equation [14]:

$$\hat{T}_L = K_P e_P + K_I \int e_P dt \quad (5)$$

$$e_P = V_{ds}^s (\hat{i}_{ds}^e - i_{ds}^e) + V_{qs}^s (\hat{i}_{qs}^e - i_{qs}^e) \quad (6)$$

Estimation of rotor speed is acquired from estimated stator current, rotor flux and the estimated load torque as:

$$\hat{\omega}_r = \left(\frac{3}{2}\right) \left(\frac{n_p}{J}\right) \left(\frac{L_m}{L_r}\right) [\hat{\phi}_{dr}^s \hat{i}_{qs}^s - \hat{\phi}_{qr}^s \hat{i}_{ds}^s] - \frac{\hat{T}_L}{J} \quad (7)$$

Where n_p is the no. of pole pairs and J is of inertia of motor load system (kg.m^2). The speed estimation methods in EKF and Luenberger observer always desires some correction term in order to follow speed changes. This results in the estimation always lagging the actual values. In natural observer, the speed estimation follows the speed changes simultaneously even for sudden change occurs in the load torque.

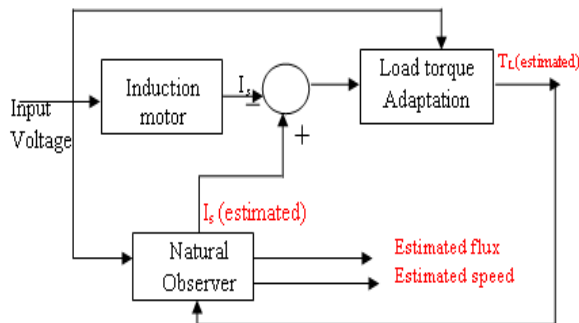


Figure 1. Block diagram of a natural observer with load torque adaptation

The closed loop arrangement of induction motor drive with natural observer is shown in Figure 2. The reference currents i_{ds}^* and i_{qs}^* are calculated as follows:

$$i_{qs}^* = \frac{L_r}{n_p L_m \hat{\phi}_r} T_e^* \quad (8)$$

i_{ds}^* is obtained by comparing the actual flux with the reference flux and the error is processed in the PI controller which gives the desired value of i_{ds}^* . It is also attained by the following equation for a known flux value.

$$i_{ds}^* = \frac{\phi_{dr}^*}{L_m} \tag{9}$$

The reference currents are transformed into stationary reference frame by rotor angle θ_e . The two phase dq-axes stator currents are transformed into three phase reference currents by 2 to 3 conversion blocks (inverse Clarke’s transformation).

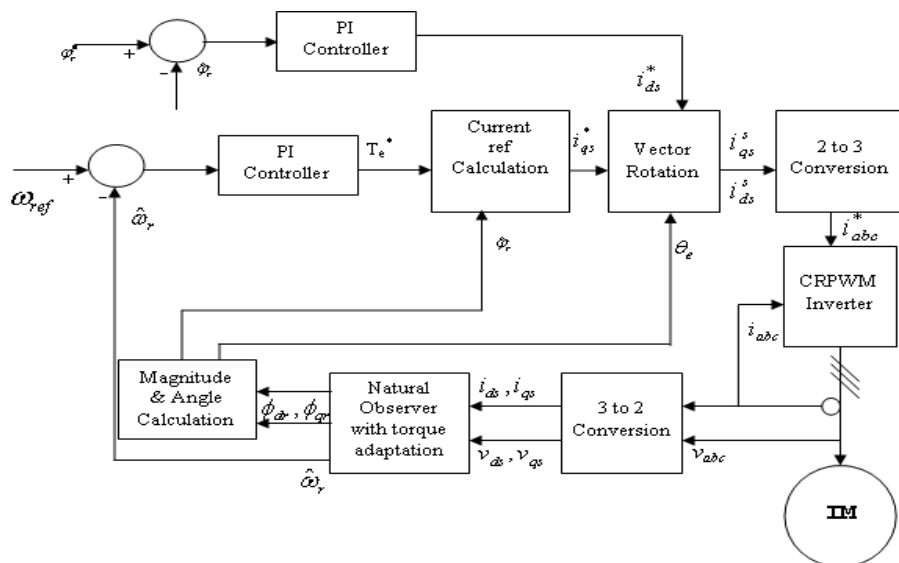


Figure 2. Closed loop arrangement of induction motor with natural observer

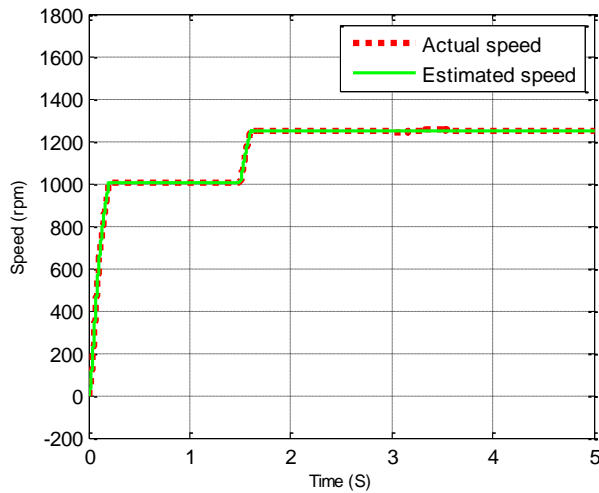
3. Simulation Results and Discussions

The simulation blocks of sensorless vector control are constructed in MATLAB using power system block sets and simulink libraries. The simulation results are presented for various running conditions. The ratings and parameters of the induction motor used for simulation are given in Table 1. Three phase squirrel cage induction motor of 0.746 kW (1HP) is used for simulation. Direct field oriented sensorless vector control scheme is used and the rotor angle is calculated from the estimated rotor fluxes. Figure 3 shows the simulation diagram of natural observer based sensorless vector control with PI controller. Induction motor and natural observer state equations are constructed in m-file and called back in simulink model file. In addition, various simple blocks available in simulink are used to construct the entire system. PI controller is constructed using PID block available in simulink libraries.

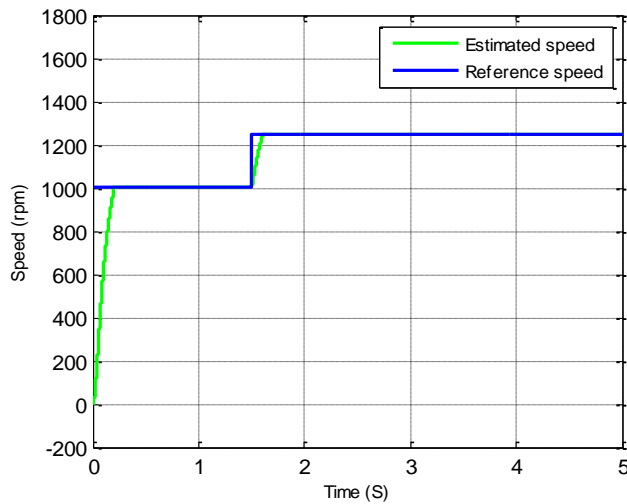
Simulations are carried out at a speed of 1000 rpm and the simulation results are shown in Figure 4. The motor is at no load at the time of starting. The command speed is set at 1000 rpm. At $t = 1.5s$, a step command is given and the speed of the motor increases from 1000 rpm to 1250rpm. At $t=3s$, a load of 2.5 Nm is applied. At steady state, the difference between estimated and actual speed is zero. The estimated and actual speed responses are shown in Figure 4 (a). It is observed that the estimated speed follow the actual speed and its convergence rate is fast even for a sudden change in load conditions. The estimated torque response is illustrated in Figure 4 (b). The estimated torque follows the load torque and no limiter is placed in the torque estimator. It is concluded that the observer estimates the speed and load torque of the motor for a variety of running conditions.

Table 1. Rating and Parameters of Induction Motor

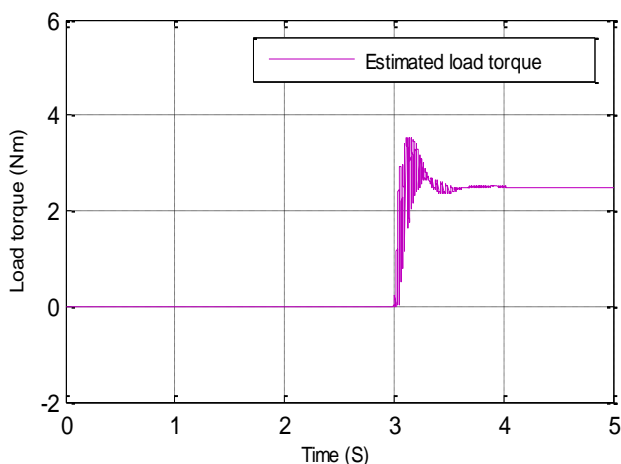
Motor rating			
Output	745.6 W	R_s	19.355 Ω
Poles	4	R_r	8.43 Ω
Speed	1415 rpm	L_s	0.715 H
Voltage	415 V	L_r	0.715 H
Current	1.8 A	L_m	0.689 H
Connection	Star	f	50 Hz



(a) Estimated and actual speed response for a reference speed of 1000 rpm and 1250 rpm



(b) Estimated speed response for a reference speed of 1250 rpm



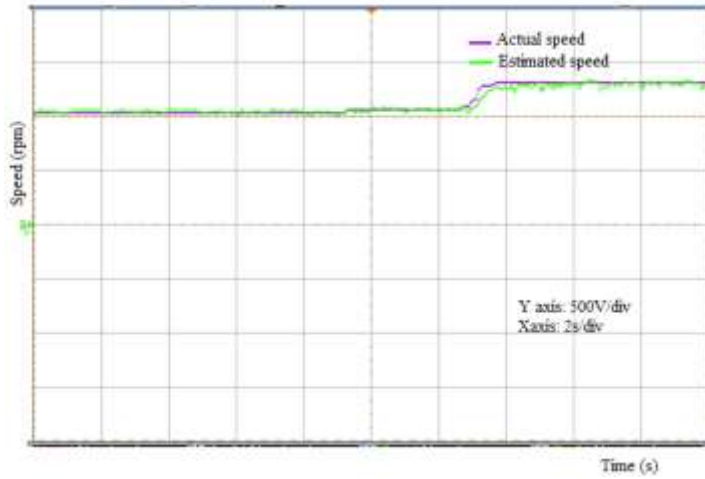
(c) Estimated load torque with 2.5 Nm load

Figure 4. Simulation results for a speed of 1000 rpm and 1250 rpm with 2.5 Nm load.

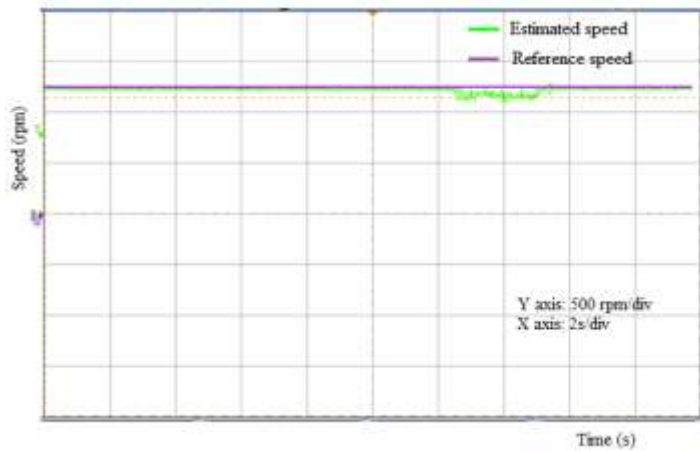
4. Hardware Results and Discussions

Three-phase squirrel cage induction motor of 745.6 W (1HP) is used for both simulation and hardware set up. Brake drum arrangements are provided for mechanical loading. The central processor unit is the TMS320F2812 DSP processor and it executes all the mathematical calculations. Various simulink blocks like natural observer and PI controllers are built in VISSIM. TMS320F2812 DSP processor supporting blocks are available in VISSIM. In VISSIM, the simulation blocks are converted into C- codes using the target support for TMS320F2812 and compiled using code composer studio internally and the output file is downloaded into the DSP processor through J-tag emulator. Three numbers of LEM current sensors and voltage sensors are used to measure the phase currents and terminal voltages of induction motor respectively. The measured analog currents and voltages are converted into digital by on chip ADC with 12 bit resolution. The feedback signals are linked to DSP processor using 26 pin header and the processor estimates the stator current, rotor flux, load torque and speed. The processor also generates the required PWM pulses to enable the three phase IGBT inverter switches in the Intelligent Power Module (IPM). Highly effective over-current and short-circuit protection is realized through the use of advanced current sense IGBT chips that allow continuous monitoring of power device current. System reliability is further enhanced by the IPM's integrated over temperature and under voltage lock out protection.

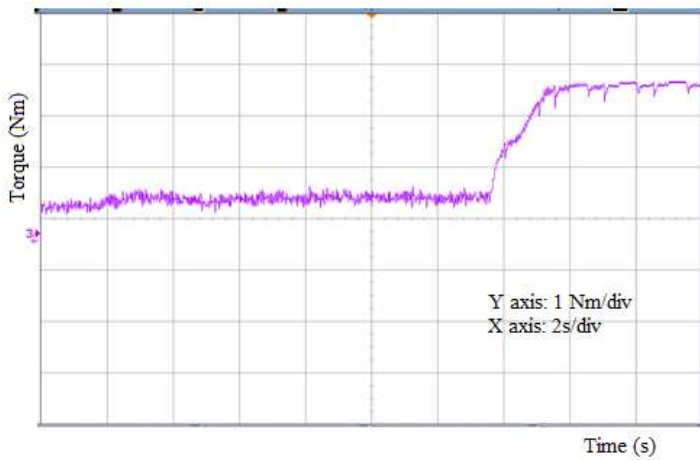
The hardware results for a step speed of 1000 rpm to 1250 rpm for a load of 2.5 Nm are shown in Figure 5. The actual speed of the motor is measured by proximity sensor. The estimated speed and actual speed waveforms are depicted in Figure 5 (a). It is identified that the estimated speed follows the actual speed and matches with the simulation waveform. The estimated speed response with respect to the reference speed of 1250 rpm is illustrated in Figure 5(b). The motor runs at a constant speed of 1250 rpm ($1\text{cm} = 500\text{rpm}$) with a load of 2.5 Nm ($1\text{cm} = 1\text{Nm}$). The external load is applied by brake drum mechanism and the torque is calculated using standard formula. The estimated torque waveform observed under no load and a load of 2.5 Nm is illustrated in Figure 5(c) and it follows the applied load. The dq-axes stator current waveform obtained by simulation and hardware results are shown in Figure 6. It is inferred that the hardware results support the simulation results.



(a) Estimated and actual speed response for a step speed of 1000 rpm to 1250 rpm

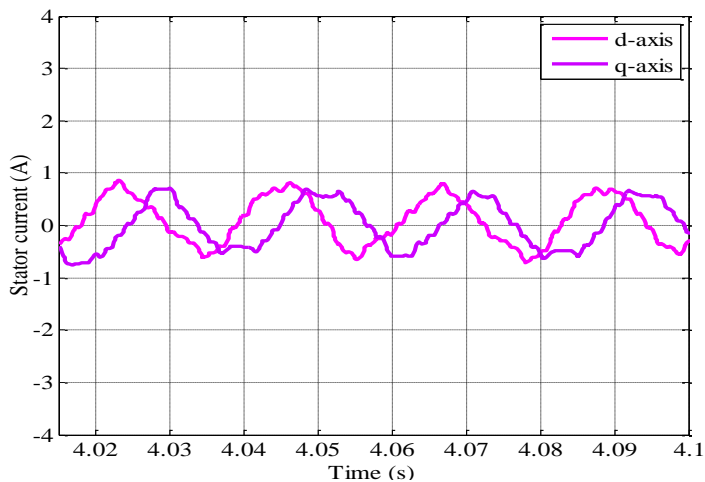


(b) Estimated speed response for a reference speed of 1250 rpm

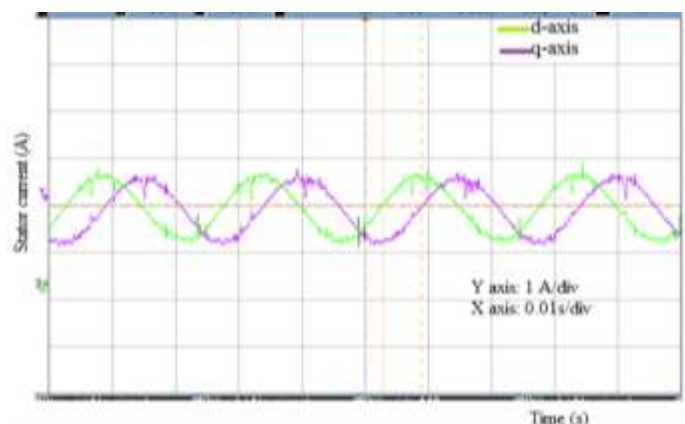


(c) Estimated torque with 2.5 Nm load

Figure 5. Experimental results for a speed of 1000 rpm and 1250 rpm with 2.5 Nm load



(a) dq-axes current waveform – simulation results



(b) dq-axes current waveform – hardware results

Figure 6. dq-axes stator current waveform for a speed of 1000 rpm and 1250 rpm with 2.5 Nm load

5. Conclusions

The induction motor and natural observer are modeled in MATLAB with state space model and simulations are carried out for different running conditions. It is concluded that the estimated parameters such as rotor speed and load torque follow the command value and the error is zero at steady state. The ripple is very less in the estimated torque and the convergence rates are very fast. P-I controllers are applied in the speed control loop to generate the torque reference and to maintain the rotor flux constant. Hardware results are presented to validate the performance of the natural observer and it matches with the simulation results. The natural observer is a simple and speedy estimator for sensorless vector control of induction motor drive.

6. References

- [1]. B. K. Bose, "Modern Power Electronics and AC Drives", Upper Saddle River, NJ: Prentice-Hall, pp.348-350, 2001.
- [2]. H. Kubota, K. Matsuse, and T.Nakano, "New adaptive flux observer of induction motor for wide speed range motor drives," in Proc. *IEEE IECON'90*, vol.2, 1990, pp.921-926.

- [3]. H. Kubota and K. Matsuse, "Speed sensorless field-oriented control of induction motor with rotor resistance adaptation," *IEEE Trans. Industry Applications*, vol. 30, pp. 1219–1224, Sept./Oct. 1994.
- [4]. T. Yamada, K. Matsuse and K. Sasagawa, "Sensorless control of direct field oriented induction motor operating at high efficiency using adaptive rotor flux observer", in Proc. *IEEE*, 1996, pp.1149-1154.
- [5]. K. Matsuse, Y.Kouno, H.Kawai and J.Oikawa, "Characteristics of speed sensor-less vector controlled dual induction motor drive connected in parallel fed by a single Inverter", *IEEE Trans. Industry Applications.*, vol. 40, pp. 153-161, Jan./Feb. 2004.
- [6]. K. Matsuse, Y. Kouno, H. Kawai and S. Yokomizo, "A Speed-sensor-less vector control method of parallel-connected dual induction motor fed by a single inverter," *IEEE Trans. Industry Applications*, vol. 38, pp. 1566–1571, Nov./Dec. 2002.
- [7]. Maurizio Cirrincione, Marcello Pucci, Giansalvo Cirrincione and Gérard-André Capolino, "An Adaptive Speed Observer Based on a New Total Least-Squares Neuron for Induction Machine Drives", *IEEE Trans. Industry Applications*, vol. 42, no. 1, pp.89 - 104, January/February 2006.
- [8]. Luigi Salvatore, Silvio Stasi, and Lea Tarchioni, "A new EKF-based algorithm for flux estimation in induction machines", *IEEE Trans. Industrial Electronics*, vol.40, no.5, pp.496-504, October 1993.
- [9]. Y.R. Kim, S.K. Sul and M.H. Park, "Speed sensorless vector control of induction motor using Extended Kalman Filter", *IEEE Trans. Industry Applications.*, vol. 30, no. 5, pp.1225-1233, September / October 1994.
- [10]. H.W. Kim and S.K. Sul, "A New motor Speed Estimator Using Kalman Filter in Low-Speed range", *IEEE Trans. Industry Applications*, vol. 43, no. 4, pp.498-504, August 1996.
- [11]. K. L. Shi, T. F. Chan, Y. K. Wong and S. L. Ho, "Speed estimation of an induction motor drive using an optimized Extended Kalman Filter", *IEEE Trans. Industrial Electronics*, vol. 49, pp. 124-133, Feb. 2002.
- [12]. M. Barut, S. Bogosyan and M. Gokasan, "Speed-sensorless estimation for induction motors using Extended Kalman Filters", *IEEE Trans. Industrial Electronics*, vol. 54, no.1, pp. 272-280, Feb. 2007.
- [13]. M. Barut, S. Bogosyan and M. Gokasan, "Experimental evaluation of Braided EKF for sensorless control of induction motors", *IEEE Trans. Industrial Electronics*, vol. 55, no.2, pp. 620-632, Feb. 2008.
- [14]. M. Tsuji , Y. Umesaki , R. Nakayama , and K. Izumi, "A Simplified MRAS based sensorless vector control method of induction motor", in proc. *IEEE*, 2002, pp.1090-1095.
- [15]. Mohamed Rashed, Fraser Stronach and Peter Vas, "A Stable MRAS-based sensorless vector control induction motor drive at low speeds", in proc. *IEEE*, 2003, pp. 1181-1188.
- [16]. R. Cardenas, R. Pena, G. Asher, J. Clare and J. Cartes, "MRAS observer for doubly fed induction machines", *IEEE Trans. Energy Conversion*, vol.19, no.2, pp. 467-468, June 2004.
- [17]. M. Cirrincione, M. Pucci, G. Cirrincione and G. A. Capolino, "A new TLS-based MRAS speed estimation with adaptive integration for high- performance induction machine drives", *IEEE Trans. Industry Applications*, vol. 40, no.4, pp.1116-1137, July/Aug. 2004.
- [18]. M. Cirrincione and M. Pucci, "An MRAS-based sensorless high-performance induction motor drive with a predictive adaptive model", *IEEE Trans. Industrial Electronics*, vol. 52, no.2, pp. 532-551, April 2005.
- [19]. S. R. Bowes, A. Sevinc and D. Holliday, "New natural observer applied to speed sensorless DC servo and induction motors", *IEEE Trans. Industry Applications*, vol. 51, no.5, pp. 1025–1032, Oct. 2004.
- [20]. J. Guzinski, M. Diguët, Z. Krzeminski, A. Lewicki and H. Abu-Rub, "Application of speed and load torque observers in high- speed train drive for diagnostic purposes", *IEEE Trans. Industry Applications*, vol. 56, no. 1, pp.248-256, Jan. 2009.

- [21]. J. Guzinski and H. Abu-Rub, M. Diguët, Z. Krzeminski and A. Lewicki “Speed and load torque observer application in high speed train electric drive”, *IEEE Trans. Industry Applications*, vol. 57, no. 2, pp.565-574, Feb. 2010.
- [22]. Adnan Derdiyok, “Speed-Sensorless Control of Induction Motor Using a Continuous Control Approach of Sliding-Mode and Flux Observer”, *IEEE Trans. Industry Applications*, vol. 52, no. 4, pp.1170-1176, August 2005.
- [23]. C. Lascu and G.D. Andreescu, “Sliding mode observer and improved integrator with DC-offset compensation for flux estimation in sensorless controlled induction motors”, *IEEE Trans. Industrial Electronics*, vol. 53, no.3, pp.785-794, Feb.2006.

APPENDIX

NOMENCLATURE

R_s, R_r	Stator and rotor resistance (Ω) respectively	i_{ds}^s, i_{qs}^s	d-axis and q-axis stator current in stator reference frame (A)
L_s, L_r	Stator and rotor self inductance (H) respectively	$\hat{i}_{ds}^s, \hat{i}_{qs}^s$	Estimated d-axis and q-axis stator current in stator reference frame (A)
J	Inertia of the motor load system. ($\text{Kg}\cdot\text{m}^2$)	V_{ds}^s, V_{qs}^s	d-axis and q-axis stator voltage in stator reference frame (V)
τ_r	Rotor time constant	$\varphi_{dr}^s, \varphi_{qr}^s$	d-axis and q-axis rotor flux in stator reference (Wb)
σ	Leakage co-efficient	$\hat{\varphi}_{dr}^s, \hat{\varphi}_{qr}^s$	Estimated d-axis and q-axis rotor flux in stator reference frame (Wb)
“^”	Represents estimated values	T_L	Load torque (Nm)
A	State matrix	\hat{T}_L	Estimated load torque (Nm)
X	State vector	T_e	Electromagnetic torque developed (Nm)
B	Input matrix	ω_r	Rotor angular velocity (rad/s)
V_s	Input vector	$\hat{\omega}_r$	Estimated rotor angular velocity (rad/s)
C	Output matrix.	n_p	No. of pole pairs



R. Gunabalan obtained his B.E. degree in Electrical and Electronics Engineering from Manonmanium Sundaranar University, Tirunelveli, TamilNadu in 2000 and M.Tech. degree in Electrical Drives and Control from Pondicherry University in 2006. He did his Ph.D from Anna University, Chennai, TamilNadu in 2015. He is working as an Associate Professor in the School of Electrical and Electronics Engineering, VIT University-Chennai, TamilNadu, India. He has published / presented around 30 papers in National and International Journals / Conferences. His research

interests are in the areas of dc-dc power converters and estimation and control of induction motor drives. He is a life member of ISTE and a member of IEEE.



V. Subbiah obtained his BE (Electrical) degree from Madras University, India in 1965, ME (Control Systems) from Calcutta University in 1968 and PhD (Power Electronics) from Madras University in 1981.

He has been associated with Technical Education for more than four decades. He worked at PSG College of Technology, Coimbatore, India in various capacities and retired in May 2000. Then, he joined the Faculty of Engineering, Multimedia University, Malaysia in June 2000 on a contract appointment for two years. After returning to India, he joined Sri Krishna

College of Engineering and Technology, Coimbatore in August 2002 as the Dean of Electrical Sciences and continued in that capacity till 2013. Currently, he is working as a visiting professor at PSG College of Technology, Coimbatore.

Dr Subbiah has taught undergraduate as well as postgraduate courses for more than 40 years. He has published / presented around 80 papers in National and International Journals / Conferences.

He is a Senior Member of IEEE (USA), a Fellow of the Institution of Engineers (India), and a Life Member of Indian Society for Technical Education. His area of interest includes Power Electronics, Electrical Drives and Control Systems.